VINGNANAM Journal of Science

Journal homepage: https://journal.jfn.ac.lk/vingnanam/

Green synthesis of copper oxide and zinc oxide nanoparticles from *Spondias dulcis* leaf extract and their application for the removal of toxic methylene blue dye residue from water bodies

S. Keerththana*, R. Srikaran

Department of Chemistry, Faculty of Science, University of Jaffna, Sri Lanka

Received: 15 September 2025; Revised: 15 October 2025; Accepted: 26 October 2025

ABSTRACT

Wastewater from the textile industry is a major source of water contamination, primarily due to its high concentration of residual dyes. Even in small quantities, these dyes are toxic, mutagenic, and carcinogenic, posing significant risks to both aquatic life and human health. This has led to an urgent need for the development of cost-effective and sustainable methods for water purification. In a recent study, copper oxide (CuO) and zinc oxide (ZnO) nanoparticles were synthesised using a method with *Spondias dulcis* leaf extract. Acetate salts were added to a basic medium (pH 12) leaf extract, and the mixture was stirred, centrifuged, and then calcined at 400°C for two hours. The resulting nanoparticles were characterized using UV-Visible spectroscopy, Fourier Transform Infrared (FTIR) spectroscopy and X-ray Diffraction (XRD) technique. UV-Visible analysis confirmed the presence of ZnO nanoparticles with a peak at 365 nm and CuO nanoparticles with a peak at 345 nm. FTIR analysis indicated that phytochemicals from the plant extract played a role in the synthesis and from XRD results indicated that synthesized ZnO and CuO nanoparticles were hexagonal and monoclinic with 18.71 and 21.90 nm, respectively. The nanoparticles were tested for their ability to degrade Methylene Blue (MB) dye. CuO nanoparticles proved to be more effective, achieving a 96.2% degradation rate, while ZnO nanoparticles reached 92%. The optimal conditions for dye removal were identified as follows: a pH of 12, a dye concentration of 10 ppm, a contact time of 90 minutes, a nanoparticle dosage of 0.2 g/L, and a temperature of 45°C. This research highlights a promising, eco-friendly approach to cleaning dye-contaminated water.

Keywords: Green synthesis, CuO nanoparticles, ZnO nanoparticles, Methylene blue dye

1.0 INTRODUCTION

Water pollution has emerged as a major environmental challenge over the past few decades, largely due to the discharge of industrial wastewater containing heavy ions and reactive dyes. The widespread use of organic dyes in industries like textiles, paper, pharmaceuticals, food, and cosmetics contributes significantly to this problem, prompting researchers to develop solutions for wastewater treatment[1].

The discharge of substantial quantities of these chemical compounds into wastewater streams leads to significant problems for aquatic organisms, ecosystems, and human populations. Dyes are broadly categorized into cationic, anionic, and non-ionic types[2]. The removal of cationic dyes is particularly difficult because they are highly water-soluble and impart very vibrant colours to water bodies[3]. As the global population continues to grow, along with the development of more limited resources due to the energy crisis and environmental degradation, the pollution of the environment and its threat to human well-being have become more pronounced. Chemically contaminated dye

* siva24keerthy@gmail.com

wastewater is a serious concern for human health, being toxic, carcinogenic, allergenic, and teratogenic. Consequently, the presence of dye wastewater poses a growing risk to the safety of our water supply[4]. Methylene blue, a cationic azo dye widely used in the paint, textile, paper, and printing industries, is a prime example. If it is released into the environment without adequate treatment, it can cause various health problems, including vomiting, eye burns, skin irritation, respiratory issues, mental disorders, excessive sweating, and severe damage to the central nervous system[5].

The removal of Methylene blue and other dyes from wastewater is more critical than ever. A wide range of physical, chemical, and biological methods have been developed to treat dye-contaminated water, including adsorption, coagulation, membrane separation, chemical oxidation, electrochemical treatment, and microbial degradation[6]. Industries are now adopting innovative, rapid, and sustainable processes to improve wastewater colour removal. This effort is driven by increasingly strict laws and regulations regarding the discharge of colored effluents[7].

While methods like physical separation (e.g. membrane filtration) and various chemical treatments are effective at reducing dye, organic, and inorganic pollutants, their high operational and maintenance costs often make them impractical for large-scale applications[8]. This has created a demand for alternative technologies that are not only efficient and effective but also inexpensive, eco-friendly, and cost-effective for treating liquid dye waste.

Photocatalytic degradation has emerged as a promising technique for removing organic dye pollutants, valued for its environmental friendliness and for not generating secondary pollutants. This method relies on the use of a catalyst and light to break down harmful compounds[9]. To enhance this process, researchers are increasingly turning to nanotechnology, a field with wide-ranging applications in various scientific disciplines.

Specifically, nanoparticles (NPs), which are particles with a size of 1–100 nm, have proven to be highly effective[10]. Among the well-studied nanomaterials for environmental engineering are copper oxide (CuO) and zinc oxide (ZnO) nanoparticles. Due to their superior physicochemical properties, CuO and ZnO are widely used as catalysts and for water treatment[11]. While various methods exist for synthesizing these nanoparticles including microwave heating, precipitation, and sol-gel synthesis, the green synthesis method via Phyto-reduction and stabilization stands out. This approach, which utilizes plant extracts, is the most environmentally friendly, cost-effective, and simplest way to produce these nanoparticles. It aligns perfectly with the goals of developing sustainable and efficient wastewater treatment solutions[12].

Building on the discussion of nanotechnology, a key application is photocatalytic activity, a process where a photocatalyst (typically a semiconductor) and light work together. This interaction generates reactive species, such as hydroxyl radicals or superoxide species, which break down organic dye molecules[13].

ZnO NPs have been identified as excellent photocatalysts for this purpose. They are a highly stable and efficient alternative to titanium dioxide (TiO2) because they have similar band gap energies. ZnO NPs' photocatalytic activity is further enhanced by oxygen vacancies, which narrow the band gap and improve their performance under visible light[14].

As a semiconductor, ZnO has a wide band gap of 3.37 eV and a large excitonic binding energy of 60 MeV[15]. In its nanoparticle form, it is non-toxic and has a high surface-area-to-volume ratio, making it ideal for many applications. These unique electrical, chemical, and optical properties are why ZnO NPs are used in diverse fields, including photocatalytic degradation, solar cells, LEDs[16], and drug delivery, as well as in devices like acoustic wave and transparent electrodes.

To complement the properties of ZnO, other materials are also effective for the degradation of organic dyes. Light-active materials with large surface areas are crucial for this process. Several metal oxides and semiconductors

function as active photocatalysts under sunlight, primarily because of their small band gaps, low toxicity, and easy availability[17].

Among these materials, copper oxide (CuO) stands out. As a p-type semiconductor, it has a narrow band gap of 2.1 to 2.71 eV, making it an effective photocatalyst. CuO is a fundamental copper compound with a variety of useful physical properties[18]. Its superior catalytic capabilities make CuO nanoparticles (NPs) the most frequently used metal nanoparticles for wastewater treatment. The material is also vital to other industries, including those involving gas sensors, high-temperature superconductors, and solar energy conversion.

This study utilizes the *Spondias dulcis* plant, also known as ambarella or Otaheite apple, for the synthesis of CuO and ZnO NPs. The plant is well known for its various uses; its ripe fruit is consumed raw or processed into juices and jams, while its young leaves are used for seasoning, and its mature leaves in salads.

Beyond its culinary applications, *S. dulcis* has a long history in traditional medicine. In Cambodian folk medicine, the bark is used to treat diarrhea[19]. The fruit has been traditionally used to relieve itchiness, internal ulceration[20], sore throats, and skin inflammation, and to improve eyesight and treat eye infections. These medicinal properties suggest the presence of a rich array of phytochemicals within the plant, which are key to facilitating the green synthesis of the nanoparticles. The use of this plant extract aligns with the goal of creating an environmentally friendly, cost-effective, and non-toxic method for nanoparticle production[21].

2.0 MATERIALS AND METHODOLOGY

2.1 Preparation of leaf extract

Spondias dulcis were collected from the Jaffna peninsula. They were thoroughly washed under running tap water then in distilled water and following this dried in the shade for 10 days. Then these dried plant materials were cut into small pieces using stainless steel scissors. Then they were labelled and stored in air-sealed polythene bags separately for further use. For the preparation of the leaf extract of *Spondias dulcis,* 10 g of dried leaves were weighted separately, and they were transferred into a 500 mL beaker. Then 100 mL of distilled water was added to each beaker and warmed at 50 °C for 1 hour. After cooling down, they were filtered through suction using Whatman No.1 filter paper. The leaf extracts were stored in the refrigerator at 4 °C for further usage[22].

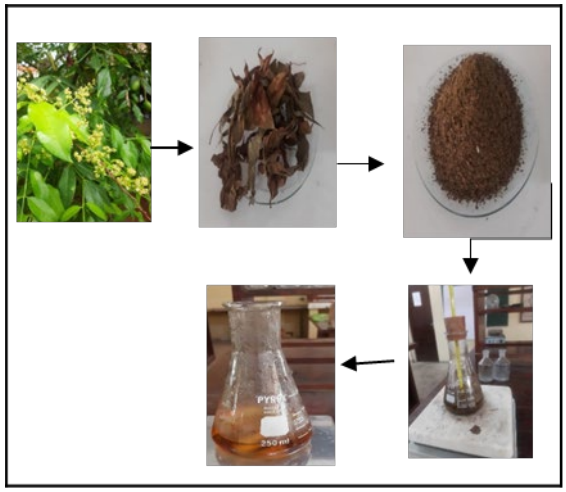

Figure 1. Preparation process of *Spondias dulcis* leaf extraction

2.2 Synthesis of Zinc oxide nanoparticles (ZnO NPs)

0.1 M zinc acetate solution was stirred for one hour at 45°C. Then 2 M NaOH was added until a pH of 12 was obtained. 10 mL of leaf extract was added to 40 mL of salt solution. It was stirred for 2 hours (orangish brown to light brown). After that, it was cooled to room temperature. That solution was centrifuged at 7500 rpm for 15 min. it was washed and again centrifuged. It was dried in oven at 80 °C and calcination at 500 °C for 1 hour[23].

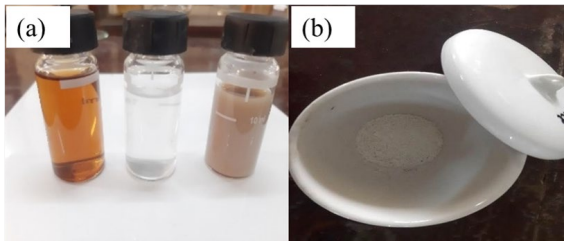

Figure 2. (a) colour change of solution during ZnO NPS synthesis, (b) ZnO NPs

2.3 Synthesis of Copper oxide nanoparticles (CuO NPs)

0.1 M copper acetate solution was stirred for one hour at 45°C. Then 2 M NaOH was added until get a pH of 12. 10 mL of leaf extract was added to 40 mL of salt solution. It was stirred for 2 hours (blue to black). After that it was cooled to room temperature. That solution was centrifuged at 7500 rpm for 15 min. It was washed and again centrifuged. It was dried in an oven at 80 °C and calcination at 500 °C for 1 hour[24].

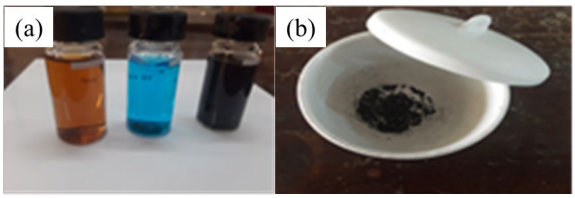

Figure 3. (a) colour change of solution during CuO NPS synthesis, (b) CuO NPs

2.4 Characterization of ZnO and CuO NPs

2.4.1 UV-Vis spectroscopy analysis

Samples of synthesis CuO and ZnO NPs (1 mL) of the suspension were collected to monitor the completion of bio reduction in an aqueous solution, followed by dilution of the samples with 3 mL of deionized water and subsequent scan in UV-visible spectra, between wavelengths of 350 to 700 nm in a spectrophotometer (Model-Jasco V-570).

2.4.2 FTIR and XRD analysis

The samples of CuO and ZnO nanoparticles were centrifuged (HERMLE-Z 287A) at 7,500 rpm for 20 minutes to isolate the nanoparticles from free proteins or other compounds present in the solution, and the centrifuge was collected and kept for 1 hour in the oven at 80 °C and finally calcined at 500 °C then it was used for FTIR and XRD analysis[25].

2.4.3 Methylene blue degradation

In this study, batch experiments were conducted to investigate how various parameters influence MB dye degradation. In the experiment, MB dye concentration (10–40 ppm), pH (4-12), and solution temperature (25–55 ˚C) were varied one at a time. For pH adjustment, NaOH or HCl solutions were used. A UV–vis spectrometer was used to measure dye concentrations.

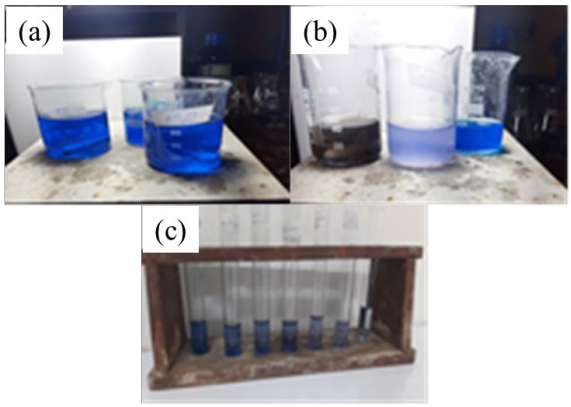

Figure 4. (a) Initial stage of dye removal, (b) during degradation process, (c) initial to final degraded dye

2.4.4 Optimization of MB dye concentration

Three sets of MB dye solutions (100 mL each) with four different concentrations (10, 15, 20, and 25 ppm) were prepared for ZnO and CuO nanoparticles. The pH was adjusted to 10 using sodium hydroxide. Then, 20 mg of nanoparticles were added to each solution, which was left in a dark area for 30 minutes to reach equilibrium[10]. At once a time three samples were placed under a visible light source (an LED bulb) such as a control (without nanoparticles), a sample containing ZnO nanoparticles, and a sample containing CuO nanoparticles. The solutions were stirred using a magnetic stirrer, while all other parameters were kept constant by maintaining room temperature, pH, and dose amount.

During the degradation process, 5 mL of solution was collected every 15 minutes for up to 90 minutes from each solution. The absorbance of each sample was then measured using a UV-Visible spectrophotometer.

2.4.5 Optimization of pH of MB dye solution

Three sets of MB dye solutions (100 mL each) with four different pH (4,8,10,12) were prepared for ZnO and CuO nanoparticles. The pH was adjusted by using sodium hydroxide and hydrochloric acid. Then, 20 mg of nanoparticles dark area for 30 minutes to reach equilibrium. were added to each solution, which was left in a

At once a time three samples were placed under a light source (an LED bulb) such as a control (without nanoparticles), a sample containing ZnO nanoparticles, and a sample containing CuO nanoparticles. The solutions were stirred using a magnetic stirrer, while all other parameters were kept constant by maintaining room temperature, dye concentration (10 ppm), and dose amount[26].

During the degradation process, 5 mL of solution was collected every 15 minutes for up to 90 minutes from each solution. The absorbance of each sample was then measured using a UV-Visible spectrophotometer.

2.4.6 Optimization of Temperature of MB dye solution

Three sets of MB dye solutions (100 mL each) with four different temperatures (25,30,45,55 °C) were prepared for ZnO and CuO nanoparticles. The pH was adjusted to 12 by using sodium hydroxide. Then, 20 mg of nanoparticles were added to each solution, which was left in a dark area for 30 minutes to reach equilibrium.

At once a time three samples were placed under a light source (an LED bulb) such as a control (without nanoparticles), a sample containing ZnO nanoparticles, and a sample containing CuO nanoparticles. The solutions were stirred using a magnetic stirrer, while all other parameters were kept constant by maintaining pH 12, dye concentration (10 ppm), and dose amount[8].

During the degradation process, 5 mL of solution was collected every 15 minutes for up to 90 minutes from each solution. The absorbance of each sample was then measured using a UV-Visible spectrophotometer.

3.0 RESULTS and DISCUSSION

3.1 Colour change

After the addition of *Spondias dulcis* extract to the aqueous solution of copper acetate of 0.1 M concentration, the CuO nanoparticles mixture showed a gradual change in colour at 45 °C with blue to black colour[27]. After the addition of *Spondias dulcis* extract to the aqueous solution of zinc acetate of 0.1 M concentration, the mixture of ZnO nanoparticles showed a gradual change in colour at 45 °C with orangish brown to light brown colour[28].

3.2 Characterization of ZnO and CuO NPs

3.2.1 UV – visible analysis

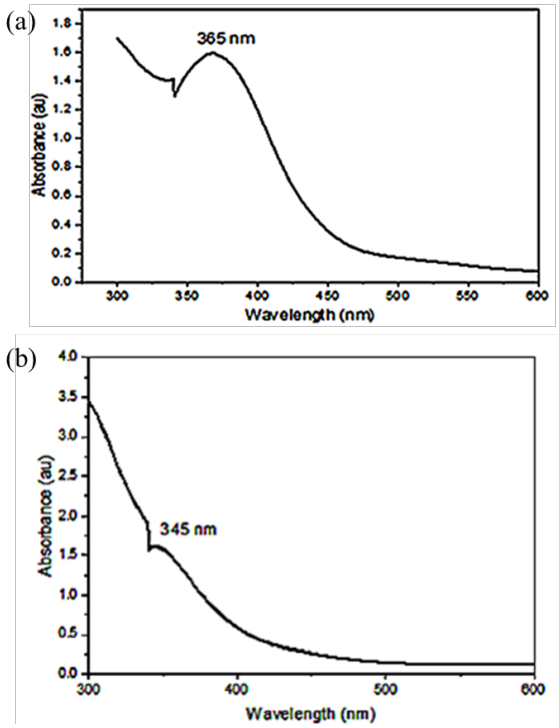

Figure 5. (a) UV -Visible spectrum of ZnO NPs, (b) UV-Visible spectrum of CuO NPs

The formation of copper oxide and zinc oxide nanoparticles were reflected in spectral data obtained by using a UV-Vis spectrophotometer. It shows absorbance peaks at 345 nm and 365 nm respectively for the CuO NPs and ZnO NPs samples[29].

3.3 FTIR analysis

3.3.1 ZnO NPs

Broad Peak around 3400 cm^{-1}-This region typically corresponds to O-H stretching vibrations. The broadness suggests the presence of hydroxyl groups (-OH) from surface-adsorbed water or hydroxyl groups attached to the ZnO nanoparticles. Region around 2800–3000 cm^{-1}: weak signals are present, they might indicate C-H stretching vibrations, potentially from organic contaminants or capping agents

used during nanoparticle synthesis. Sharp Peak around 1600 cm^{-1}: This is associated with H-O-H bending vibrations from water molecules adsorbed onto the ZnO surface. 1720 cm^{-1}: Peaks in this region could indicate stretching vibrations of C=O bonds, suggesting the presence of residual organic compounds from synthesis. Fingerprint Region (500–1000 cm^{-1}) This is the most important region for ZnO[23]. A strong absorption band around 400–600 cm^{-1} is attributed to Zn-O stretching vibrations, confirming the formation of ZnO nanoparticles.

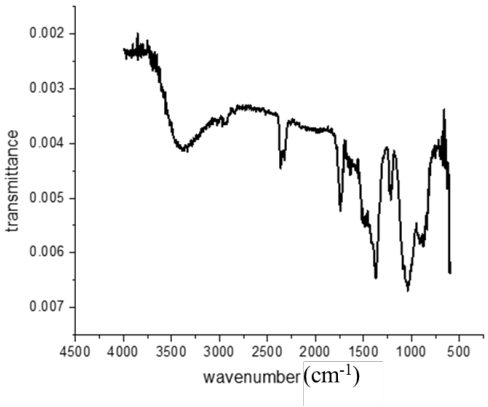

Figure 6. FTIR spectrum of ZnO NPs

3.3.2 CuO NPs

Figure 7 indicates that the biomolecules are responsible for capping and stabilizing CuO NPs. 1380 cm^{-1} polyphenols and heterocyclic components. The bands at 800–600 cm^{-1}region (for C–H out of plane bend) are characteristic of aromatic phenols. This can be attributed to the adsorption of phenolic compounds such as tannic acid products on the CuO NPs surface which may be responsible for the capping and particle stabilization[30].

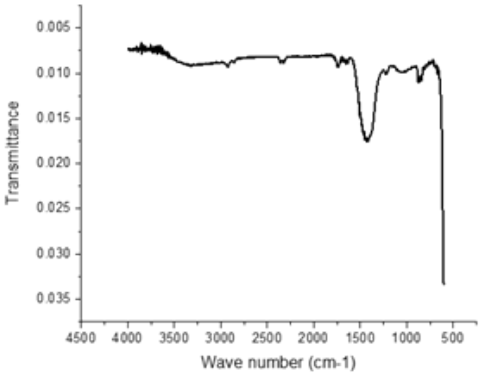

Figure 7. FTIR spectrum of CuO NPs

3.4 XRD analysis

Figure 8 shows the X-ray diffraction patterns of CuO NPs. The 2θ characteristic peaks of CuO at 32.73°, 35.74°, 38.94°, 48.99°, 53.67°, 58.43°, 61.75°, 66.44°, 68.21°, 72.56° and 75.22° corresponding to the (110), (11-1), (111), (20-2), (020), (202), (-113), (31-1), (220), (311) and (22-2) planes of the crystal lattice, respectively. The results of the XRD analysis are in accordance with JCPDS No: 96-901-5925, suggesting the typical monoclinic crystal structure with the lattice parameters a=4.68320 A°, b=3.42880 A°, c=5.12970 A°, β=99.309°and with space group C 1 2/c 1 (15)[31].

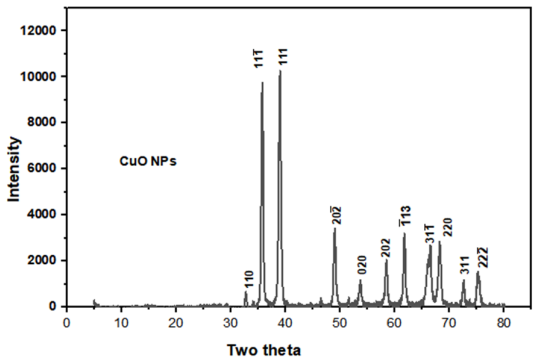

Figure 8. XRD pattern of CuO NPs

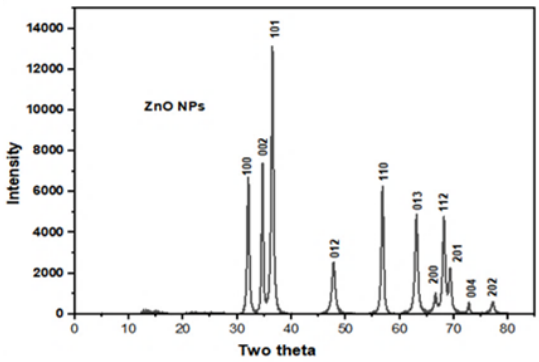

Figure 9. XRD pattern of ZnO NPs

Figure 9 shows the X-ray diffraction patterns of ZnO NPs. The 2θ characteristic peaks of ZnO at 32.03°, 34.67°, 36.50°, 47.78°, 56.83°, 63.09°, 66.62°, 68.17°, 69.31°, 72.78° and 77.16° corresponding to the (100), (002), (101), (012), (110), (013), (200), (112), (201), (004) and (202) planes of the crystal lattice, respectively. The results of the XRD analysis are in good agreement with the Joint Committee on Powder

Diffraction Standards (JCPDS) card, corresponding to JCPDS No. 96-900-8878, which suggests a typical hexagonal crystal structure with lattice parameters a = 3.24950 Å and c = 5.20590 Å, and a space group of P63mc (186) [32].

It is proposed that pure-phase hexagonal ZnO nanoparticles (NPs) and monoclinic CuO NPs were successfully synthesized through a straightforward green method. Interestingly, the synthesized ZnO and CuO nanoparticles were found to be highly crystalline, despite not undergoing any additional heat treatments. This finding indicates that our green synthesis route can produce crystalline nanomaterials simply and efficiently.

In addition, the average crystallite size of ZnO and CuO NPs were calculated using the Debye–Scherrer formula[33].

$$D = \frac{K\lambda}{\beta \cos\theta}$$

where D, K, λ, θ, and β are the crystallite size, Scherrer constant, wavelength of the X-ray source, diffraction angle, and full width at half maximum (FWHM) of the peak, respectively. The sharp and narrow diffraction peaks indicate the product is well crystalline in nature. The synthesized CuO and ZnO NPs were found to be pure, without any impurities. The average crystallite size (D) of CuO and ZnO NPs were calculated to be about 21.9020 and 18.7100 nm respectively[34].

3.5 Methylene blue degradation

Using the calibration curve and the removal percentage equation, the optimized parameters were determined[12].

$$\text{Removal } \% = \frac{Co - Ce}{Co} \times 100\%$$

Where,

Co – Initial concentration of the Methylene blue solution

Ce – final concentration of the Methylene blue solution

3.5.1 Optimization of MB dye concentration

In this study, firstly, the impact of initial dye concentration on MB dye removal by both CuO and ZnO NPs was investigated, where dose concentration, pH and contact time were considered 2 g/L, 10 and 90 min, respectively. The outcome of the study is shown in the Figure. The result reveals that the adsorption efficiency was maximum at 10 ppm of MB dye for both nanoparticles[25].

Dye concentration is a critical factor in catalytic treatment, as it directly impacts the amount of dye adsorbed and removed. In this study, different concentrations of methylene blue (MB) dye, ranging from 10-25 ppm, were tested. The results showed that the maximum decolorization of the MB dye occurred at a concentration of 10 ppm.

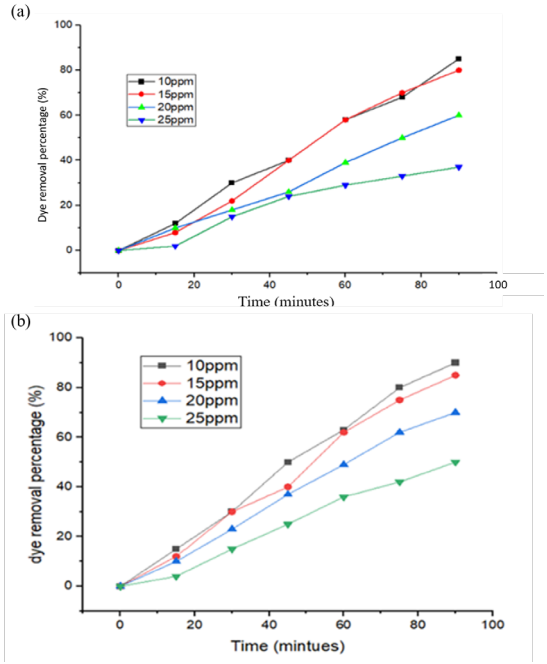

Figure 10. (a) Optimization of concentration in ZnO NPs, (b) optimization of concentration in CuO NPs

Increasing the dye concentration beyond this point led to a decrease in decolorization. This is because a higher number of dye molecules can cause self-association, making the solution turbid[35]. Furthermore, an excessive concentration of the dye molecules can inhibit the catalytic sites on the nanoparticles, thereby slowing down the reaction rate. Similar observations have been made in other studies, such as the biodegradation of disperse yellow dye, where increased concentration led to reduced effectiveness due to solution turbidity and substrate inhibition.

3.5.2 Optimization of pH of MB dye solution

To identify the optimal pH for efficient methylene blue photodegradation, experiments were conducted at various pH levels (4,8,10,12). The catalyst load and dye concentration were held constant. The results, illustrated in Figure 11, showed that degradation was most effective in a basic environment, with the highest degradation rate recorded at pH 12. This finding is consistent with prior research[36].

The pH of the solution is one of the critical factors in determining the efficacy of dye removal through adsorption, as it influences the surface charge of the adsorbent. The figure shows that efficiency increase with pH increasing thus optimal pH for maximum efficiency was determined to be 12, as at this pH, the surface of the nanoparticles will be negatively charged in the solution, allowing for high removal efficiency towards MB, which is a cationic dye, through electrostatic attraction between the negatively charged adsorbent and cationic MB.

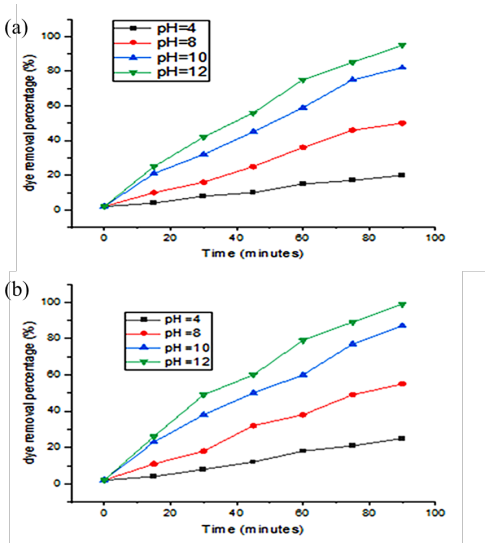

Figure 11. Optimization of pH in ZnO NPs, (b) Optimization of pH in CuO NPs

The presence of electrostatic interaction was also evident from FTIR analysis, which suggested that O–H, and C=O groups in cellulose, hemicellulose, and lignin of the nanoparticle's adsorbent played a role in initiating this interaction[37].

3.5.3 Optimization of Temperature of MB dye solution

The impact of temperature on MB dye adsorption was also investigated, and the results are presented in Figure 12. Investigation of the result reveals that an increase in adsorption capacity with temperature increment up to 45 °C and then further increase started decreasing tendency of the adsorption. MB dye removal efficiency was determined by varying temperature from 25 to 55 °C where dye concentration, dose concentration, contact time and pH were considered 10 ppm, 2 g/L, 90 min and 12 respectively.

The impact of temperature on MB dye adsorption was also investigated, and the results are presented in the Figure. Investigation of the result reveals that an increase in adsorption capacity with temperature increment up to 45 °C, and then further increase, shows a decreasing tendency of the adsorption. MB dye removal efficiency was determined by varying temperature from 25 °C to 55 °C, where dye concentration, dose concentration, contact time and pH were considered 10 ppm, 2 g/L, 90 min and 12, respectively

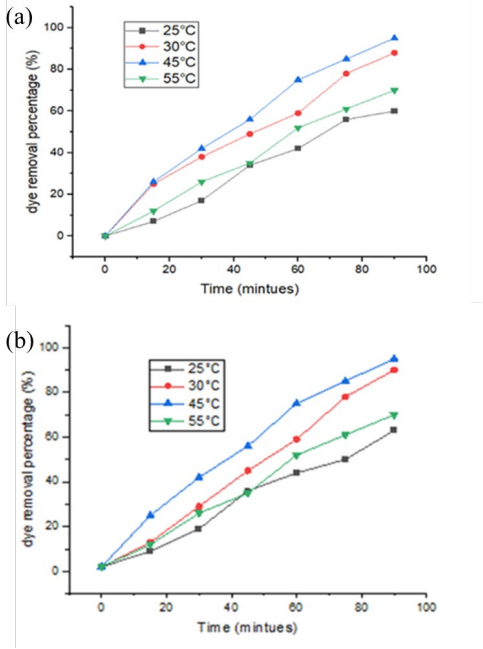

Figure 12. (a) Optimization of temperature in ZnO NPs, (b) Optimization of temperature in CuO NPs

3.5.4 Plausible Mechanism for Methylene Dye Degradation

Plausible mechanism for the removal of MB dye through the adsorbent indicating an exothermic reaction nature. This phenomenon can be attributed to the weakening of adsorptive forces between the adsorbent and dye molecules at higher temperatures, as reported in previous studies by[38].

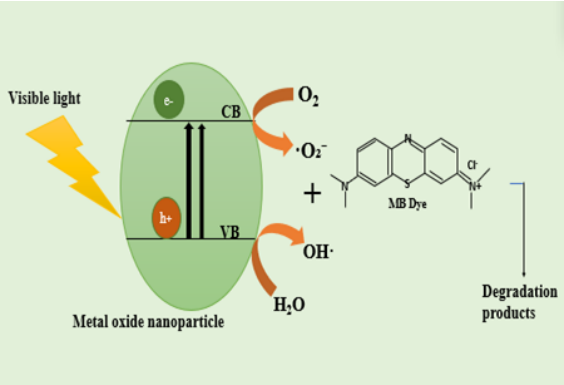

Figure 13. Schematic diagram for photocatalytic degradation process of MB dye by using nanoparticles

The decolorization of methylene blue (MB) dye is primarily caused by the interaction between hydroxyl radicals ($OH^{\cdot}$) and the dye molecules or their intermediate photoproducts. The effectiveness of this process is also influenced by the **size,** morphology, and surface charge of the synthesized nanoparticles. Nanoparticles with a controlled size and a specific surface charge can degrade dyes very efficiently. Building on the work of [39], who demonstrated the effectiveness of green-synthesized metal nanoparticles for decomposing organic dyes over time, our own green-synthesized nanoparticles also showed significant potential. They completely degraded the MB dye within 90 minutes under light irradiation. This degradation was visually confirmed as the solution changed from a deep blue to a colourless state. A possible mechanism for this photocatalytic degradation is illustrated in the schematic diagram in Figure 13.

When a heterogeneous photocatalyst is irradiated with a suitable light source, a process occurs where the light's energy, which is either comparable to or greater than the photocatalyst's band gap energy, creates electron-hole pairs. These photogenerated electron-hole pairs are primarily responsible for the degradation of the pollutant, in this case, the methylene blue (MB) dye.

The mechanism unfolds as follows: photogenerated electrons (e^{-}) in the conduction band of the zinc or copper oxide migrate to the surface. Upon reaching the surface, they react with absorbed oxygen (O_2) to generate a superoxide anion (O_2^{-}). Simultaneously, the hole (h^{+}) migrates to the surface of the photocatalyst and reacts with either water (H_2O) or a hydroxide ion (OH^{-}) to produce hydroxyl radicals ($HO^{\cdot}$). The steps involved in the complete photodegradation of MB are outlined in a corresponding equation. These active oxygen species, including O_2 play a crucial role in the photodegradation of MB dye and its conversion into harmless minerals or organic materials[40].

$ZnO + h\nu \rightarrow ZnO + e^{-} + h^{+}$

$e^{-} + O_2 \rightarrow O_2^{-}$

$h^{+} + H_2O \rightarrow OH^{\cdot}$

$O_2^{-} + OH^{\cdot} + MB \rightarrow$ Degradation products

4.0 CONCLUSSION

We aimed to synthesize metallic nanoparticles using a simple and eco-friendly procedure, unlike chemical methods. Here, we used the extract of *Spondias dulcis* as a reducing and capping agent.

Copper oxide and zinc oxide nanoparticles were successfully obtained from copper acetate and zinc acetate and *Spondias dulcis leaf* extract. Usually, the change in colour of the aqueous salt solution of a metal is indicative of metal oxide nanoparticle formation. In the present study, the formation of CuO and ZnO NPs was first confirmed by the rapid colour change of plant extracts. ZnO NPs showed the colour change from orangish brown to light brown and CuO NPs showed the colour change from blue to black. Furthermore, it was confirmed by UV-Vis spectra. CuO and ZnO NPs formed at the absorption maximum in 345 nm and 365 nm. The major functional group identification of the

synthesized metal nanoparticles was done using FTIR. FTIR analysis revealed the efficient capping and stabilization properties of these NPs. From XRD, the prepared ZnO and CuO NPs were pure and crystalline in the hexagonal phase and monoclinic with average sizes of 18.71 and 21.90 nm, respectively.

Optimization of MB dye removal was conducted by varying parameters such as pH, initial dye concentration and temperature. Results demonstrated that achieving a maximum removal efficiency of 92.7 % and 96.2 % (ZnO and CuO NP, respectively) under optimized conditions: pH 12, initial dye concentration of 10 ppm, contact time of 90 min, NP dosage of 0.2 g/L, and temperature of 45 °C.

REFERENCES

1. M. Sorbiun, E. Shayegan Mehr, A. Ramazani, and S. Taghavi Fardood, “Green Synthesis of Zinc Oxide and Copper Oxide Nanoparticles Using Aqueous Extract of Oak Fruit Hull (Jaft) and Comparing Their Photocatalytic Degradation of Basic Violet 3,” *Int. J. Environ. Res.*, vol. 12, no. 1, pp. 29–37, 2018, doi: 10.1007/s41742-018-0064-4.
2. R. A. Basit *et al.*, “Successive Photocatalytic Degradation of Methylene Blue by ZnO, CuO and ZnO/CuO Synthesized from Coriandrum sativum Plant Extract via Green Synthesis Technique,” *Crystals*, vol. 13, no. 2, 2023, doi: 10.3390/cryst13020281.
3. M. I. Din *et al.*, “Green synthesis of zinc ferrite nanoparticles for photocatalysis of methylene blue,” *Int. J. Phytoremediation*, vol. 22, no. 13, pp. 1440–1447, 2020, doi: 10.1080/15226514.2020.1781783.
4. F. A. Alharthi, A. A. Alghamdi, A. A. Alothman, Z. M. Almarhoon, M. F. Alsulaiman, and N. Al-Zaqri, “Green synthesis of zno nanostructures using salvadora persica leaf extract: Applications for photocatalytic degradation of methylene blue dye,” *Crystals*, vol. 10, no. 6, 2020, doi: 10.3390/cryst10060441.
5. M. H. Kahsay, “Synthesis and characterization of ZnO nanoparticles using aqueous extract of Becium grandiflorum for antimicrobial activity and adsorption of methylene blue,” *Appl. Water Sci.*, vol. 11, no. 2, pp. 1–12, 2021, doi: 10.1007/s13201-021-01373-w.
6. A. Fouda, S. S. Salem, A. R. Wassel, M. F. Hamza, and T. I. Shaheen, “Optimization of green biosynthesized visible light active CuO/ZnO nano-photocatalysts for the degradation of organic methylene blue dye,” *Heliyon*, vol. 6, no. 9, p. e04896, 2020, doi: 10.1016/j.heliyon.2020.e04896.
7. Modi, Shreya, Virendra Kumar Yadav, Amel Gacem, Ismat H. Ali, Dhruv Dave, Samreen Heena Khan, Krishna Kumar Yadav et al. "Recent and emerging trends in remediation of methylene blue dye from wastewater by using zinc oxide nanoparticles." *Water* 14, no. 11 (2022): 1749.
8. W. K. Essa, “Methylene Blue Removal by Copper Oxide Nanoparticles Obtained from Green Synthesis of Melia azedarach: Kinetic and Isotherm Studies,” *Chemistry (Switzerland)*, vol. 6, no. 1. pp. 249–263, 2024. doi: 10.3390/chemistry6010012.
9. K. Elumalai, S. Velmurugan, S. Ravi, V. Kathiravan, and G. A. Raj, “Bio-approach : Plant mediated synthesis of ZnO nanoparticles and their catalytic reduction of methylene blue and antimicrobial activity Bio-approach : Plant mediated synthesis of ZnO nanoparticles and their catalytic reduction of methylene blue and antimi,” *Adv. Powder Technol.*, vol. 26, no. 6, pp. 1639–1651, 2015, doi: 10.1016/j.apt.2015.09.008.
10. M. H. Kahsay, “Synthesis and characterization of ZnO nanoparticles using aqueous extract of Becium grandiflorum for antimicrobial activity and adsorption of methylene blue,” *Applied Water Science*, vol. 11, no. 2. 2021. doi: 10.1007/s13201-021-01373-w.
11. A. Ekinci, S. Kutluay, Ö. Şahin, and O. Baytar, “Green synthesis of copper oxide and manganese oxide nanoparticles from

watermelon seed shell extract for enhanced photocatalytic reduction of methylene blue," *Int. J. Phytoremediation*, vol. 25, no. 6, pp. 789–798, 2023, doi: 10.1080/15226514.2022.2109588.

12. A. R. Prasad, J. Garvasis, S. K. Oruvil, and A. Joseph, "Bio-inspired green synthesis of zinc oxide nanoparticles using Abelmoschus esculentus mucilage and selective degradation of cationic dye pollutants," *J. Phys. Chem. Solids*, vol. 127, no. December 2018, pp. 265–274, 2019, doi: 10.1016/j.jpcs.2019.01.003.
13. Catalysts Aroob, Sadia, Sónia AC Carabineiro, Muhammad Babar Taj, Ismat Bibi, Ahmad Raheel, Tariq Javed, Rana Yahya et al. Green Synthesis and Photocatalytic Dye Degradation Activity of CuO Nanoparticles
14. Sachin, Jaishree, N. Singh, R. Singh, K. Shah, and B. K. Pramanik, "Green synthesis of zinc oxide nanoparticles using lychee peel and its application in anti-bacterial properties and CR dye removal from wastewater," *Chemosphere*, vol. 327. 2023. doi: 10.1016/j.chemosphere.2023.138497.
15. K. K. Taha, M. Al Zoman, M. Al Outeibi, S. Alhussain, A. Modwi, and A. A. Bagabas, "Green and sonogreen synthesis of zinc oxide nanoparticles for the photocatalytic degradation of methylene blue in water," *Nanotechnol. Environ. Eng.*, vol. 4, no. 1, 2019, doi: 10.1007/s41204-019-0057-3.
16. R. Rathnasamy, P. Thangasamy, R. Thangamuthu, S. Sampath, and V. Alagan, "Green synthesis of ZnO nanoparticles using Carica papaya leaf extracts for photocatalytic and photovoltaic applications," *J. Mater. Sci. Mater. Electron.*, vol. 28, no. 14, pp. 10374–10381, 2017, doi: 10.1007/s10854-017-6807-8.
17. A. Nayak, J. K. Sahoo, S. K. Sahoo, and D. Sahu, "Removal of congo red dye from aqueous solution using zinc oxide nanoparticles synthesised from Ocimum sanctum (Tulsi leaf): a green approach," *Int. J. Environ. Anal. Chem.*, vol. 102, no. 19, pp. 7889–7910, 2022, doi: 10.1080/03067319.2020.1842386.
18. B. S. Muthukrishnan S, S. M. Muthukumar M, and S. K. T. Rao MV, "Catalytic Degradation of Organic Dyes using Synthesized Silver Nanoparticles: A Green Approach," *J. Bioremediation Biodegrad.*, vol. 06, no. 05, 2015, doi: 10.4172/2155-6199.1000312.
19. R. Vinayagam, S. Pai, T. Varadavenkatesan, M. K. Narasimhan, S. Narayanasamy, and R. Selvaraj, "Structural characterization of green synthesized α-Fe_2O_3 nanoparticles using the leaf extract of Spondias dulcis," *Surfaces and Interfaces*, vol. 20. 2020. doi: 10.1016/j.surfin.2020.100618.
20. "Molecules _ Samuggam, S., Chinni, S. V., Mutusamy, P., Gopinath, S. C., Anbu, P., Venugopal, V., ... & Enugutti, B. (2021). Green synthesis and characterization of silver nanoparticles using Spondias mombin extract and their antimicrobial activity against biofilm-producing bacteria. *Molecules*, *26*(9), 2681.
21. S. N. Chong and T. Hadibarata, "Adsorption of phenol red and remazol brilliant blue r by coconut shells (Cocos nucifera) and ambarella peels (spondias dulcis)," *Biointerface Res. Appl. Chem.*, vol. 11, no. 1, pp. 8564–8576, 2021, doi: 10.33263/BRIAC111.85648576.
22. D. K. Adeyemi, A. O. Adeluola, M. J. Akinbile, O. O. Johnson, and G. A. Ayoola, "Green synthesis of Ag, Zn and Cu nanoparticles from aqueous extract of Spondias mombin leaves and evaluation of their antibacterial activity," *African J. Clin. Exp. Microbiol.*, vol. 21, no. 2, pp. 106–113, 2020, doi: 10.4314/ajcem.v21i2.4.
23. E. Darvishi, D. Kahrizi, and E. Arkan, "Comparison of different properties of zinc oxide nanoparticles synthesized by the green (using Juglans regia L. leaf extract) and chemical methods," *J. Mol. Liq.*, vol. 286, 2019, doi: 10.1016/j.molliq.2019.04.108.
24. J. López-López, A. Tejeda-Ochoa, A. López-Beltrán, J. Herrera-Ramírez, and P. Méndez-Herrera, "Sunlight photocatalytic performance of zno nanoparticles

synthesized by green chemistry using different botanical extracts and zinc acetate as a precursor," *Molecules*, vol. 27, no. 1, 2022, doi: 10.3390/molecules27010006.

25. S. B. Endeshaw *et al.*, "Croton macrostachyus Leaf Extract-Mediated Green Synthesis of ZnO Nanoparticles and ZnO/CuO Nanocomposites for the Enhanced Photodegradation of Methylene Blue Dye with the COMSOL Simulation Model," *ACS Omega*, vol. 9, no. 1. pp. 559–572, 2024. doi: 10.1021/acsomega.3c06155.
26. Teshiwal Bizuayen Adamu, Aklilu Melese Mengesha, Mekuriaw Assefa Kebede, Bekalu Lake Bogale, Tadesse Walle Kassa,Facile biosynthesis of zinc oxide nanoparticles (ZnO NPs) using Lupinus albus L (Gibto) seed extract for antibacterial and photocatalytic applications,Volume10,2024,101724,ISSN2 2117156,https://doi.org/10.1016/j.rechem.20 24.101724.
27. S. Y. Sharaf Zeebaree, A. Y. Sharaf Zeebaree, O. I. Haji Zebari, and A. Y. Sharaf Zebari, "Sustainable fabrication, optical properties and rapid performance of bio-engineered copper nanoparticles in removal of toxic methylene blue dye in an aqueous medium," *Current Research in Green and Sustainable Chemistry*, vol. 4. 2021. doi: 10.1016/j.crgsc.2021.100103.
28. R. O. Aljedaani, S. A. Kosa, and M. Abdel Salam, "Ecofriendly Green Synthesis of Copper (II) Oxide Nanoparticles Using Corchorus olitorus Leaves (Molokhaia) Extract and Their Application for the Environmental Remediation of Direct Violet Dye via Advanced Oxidation Process," *Molecules*, vol. 28, no. 1, 2023, doi: 10.3390/molecules28010016.
29. M. S. H. Bhuiyan *et al.*, "Green synthesis of iron oxide nanoparticle using Carica papaya leaf extract: application for photocatalytic degradation of remazol yellow RR dye and antibacterial activity," *Heliyon*, vol. 6, no. 8, p. e04603, 2020, doi: 10.1016/j.heliyon.2020.e04603.
30. S. A. Moon, B. K. Salunke, P. Saha, A. R. Deshmukh, and B. S. Kim, "Comparison of dye degradation potential of biosynthesized copper oxide, manganese dioxide, and silver nanoparticles using Kalopanax pictus plant extract," *Korean J. Chem. Eng.*, vol. 35, no. 3, pp. 702–708, 2018, doi: 10.1007/s11814-017-0318-4.
31. J. Sharma, Sweta, C. Thakur, M. Vats, and S. K. Sharma, "Green synthesis of zinc oxide nanoparticles using neem extract," *AIP Conf. Proc.*, vol. 2220, no. 2, pp. 4309–4317, 2020, doi: 10.1063/5.0002093.
32. A. Muthuvel, M. Jothibas, and C. Manoharan, "Synthesis of copper oxide nanoparticles by chemical and biogenic methods: photocatalytic degradation and in vitro antioxidant activity," *Nanotechnol. Environ. Eng.*, vol. 5, no. 2, 2020, doi: 10.1007/s41204-020-00078-w.
33. M. Ghulam, T. Hajira, S. Muhammad, and A. Nasir, "Synthesis and characterization of cupric oxide (CuO) nanoparticles and their application for the removal of dyes," *African J. Biotechnol.*, vol. 12, no. 47, pp. 6650–6660, 2013, doi: 10.5897/ajb2013.13058.
34. T. Sinha and M. Ahmaruzzaman, "Green synthesis of copper nanoparticles for the efficient removal (degradation) of dye from aqueous phase," *Environ. Sci. Pollut. Res.*, vol. 22, no. 24, pp. 20092–20100, 2015, doi: 10.1007/s11356-015-5223-y.
35. J. Saha, A. Begum, A. Mukherjee, and S. Kumar, "A novel green synthesis of silver nanoparticles and their catalytic action in reduction of Methylene Blue dye," *Sustainable Environment Research*, vol. 27, no. 5. pp. 245–250, 2017. doi: 10.1016/j.serj.2017.04.003.
36. R. Davarnejad, A. Azizi, S. Asadi, and M. Mohammadi, "Green Synthesis of Copper Nanoparticles Using Centaurea cyanus Plant Extract: A Cationic Dye Adsorption Application," *Iran. J. Chem. Chem. Eng.*, vol. 41, no. 1, pp. 1–14, 2022, doi: 10.30492/ijcce.2020.120707.3944.
37. "Crystals _ Free Full-Text _ Green Synthesis of ZnO Nanostructures Using Salvadora Persica Leaf Extract_

Applications for Photocatalytic Degradation of Methylene Blue Dye."

38. L. David and B. Moldovan, "Green synthesis of biogenic silver nanoparticles for efficient catalytic removal of harmful organic dyes," *Nanomaterials*, vol. 10, no. 2. 2020. doi: 10.3390/nano10020202.
39. A. G. Liew Abdullah *et al.*, "Azo Dye Removal By Adsorption Using Waste Biomass: Sugarcane Bagasse," *Int. J. Eng. Technol.*, vol. 2, no. 1, pp. 8–13, 2005.
40. A. Ghaffar *et al.*, "Citrus paradisi fruit peel extract mediated green synthesis of copper nanoparticles for remediation of disperse yellow 125 dye," *Desalin. Water Treat.*, vol. 212, pp. 368–375, 2021, doi: 10.5004/dwt.2021.26684.